

## COMPACT CONDENSING HEAT EXCHANGER FOR EXHAUST GAS FROM FUEL CELL

Masahiro OSAKABE\* and Jin QUIN\*

\*Tokyo University of Marine Science & Technology, Koutou-ku, Tokyo 135-8533, Japan  
Phone & FAX +81-3-5245-7404, E-Mail osakabe@ipc.tosho-u.ac.jp

**ABSTRACT** The most part of energy losses in fuel cells is due to the heat released by the exhaust gas to atmosphere. The exhaust gas consists of air and steam with sensible and latent heat. As a lot of latent heat is included in the mixture gas, its recovery is very important to improve the power system efficiency using the fuel cell. The thermal hydraulic behavior was experimentally studied in a compact heat exchanger for the latent heat recovery from air-steam mixture gas. The compact heat exchanger consisted of staggered banks of 10(9) rows and 40 stages of bare tubes of small diameter. The parametric study varying the air mass concentration was conducted. The temperature distributions of cooling water and mixture gas and the amount of condensate were measured. Based on the previous basic studies, a thermal hydraulic prediction method was also proposed. For the condensation of steam on heat transfer tubes, the modified Sherwood number taking account of the mass absorption effect on the wall was used. The experimental results agreed well with the prediction proposed in this study.

**Keyword:** Latent Heat Recovery, Air mass concentration, Fuel Cell, Thermal-Hydraulic Prediction

### 1.INTRODUCTION

Recently, for a biological and environmental safety, clean fuels such as natural gas or hydrogen are recommended to use in the power system. As the clean fuel includes a lot of hydrogen instead of carbon, the exhaust flue gas includes a lot of steam accompanying with the latent heat. As a next power system, the fuel cells using only the hydrogen is planned and developed in worldwide. The most part of energy losses in fuel cells is due to the heat released by the exhaust gas to atmosphere. The exhaust gas consists of air and steam with sensible and latent heat. As a lot of latent heat is included in the mixture gas, its recovery is very important to improve the power system efficiency using the fuel cell.

Based on the previous basic studies, a prediction method was proposed for the design of heat exchanger to recover the latent heat in the air-steam mixture gas. The modified Sherwood number taking account of the mass absorption effect on the heat transfer tubes is used for the condensation of steam in the presence of non-condensing gas. Laminar film of condensate on the tubes is assumed to evaluate the heat resistance due to the inundation. In the calculation procedure, it is possible that the gas temperature coincides with the dew point which is the saturation temperature corresponding to the partial pressure of steam in the mixture gas. When the gas temperature decreases below the dew point, the condensation of steam in the mixture gas takes place and the latent heat increases the gas temperature until it coincides with the dew point.

For condensation from a steam-gas mixture flowing normal to horizontal rows of tubes, an approximate analogy

relation between heat and mass transfer was obtained with semi-theoretical consideration taking account of the mass absorption effect on the wall in the previous study.

$$Nu = f(Re, Pr) \quad (1)$$

$$Sh = \frac{Max(1, 2 - 1.2\omega)}{1 - w_i} f\left(Re, \frac{1}{\omega} Sc\right) \quad (2)$$

$$\text{where } \omega = \frac{1 - w_f}{1 - w_i}$$

Equations (1) and (2) are heat transfer and mass transfer correlations, respectively. The mass transfer equation can be derived if the heat transfer function of Nu is known. These correlations gave good predictions when the non-condensing gas fraction was more than 75% [1-10] in single and multiple stages of heat transfer tubes using actual flue gas. Also at the non-condensing gas fraction less than 75%, the good predictions were obtained in the experiment of single stage using air-steam mixture [11]. It is very important to verify the availability of the analogy relation in the heat exchanger configuration at the non-condensing gas fraction less than 75%.

The compactness can be obtained in the heat exchanger for the latent heat recovery when bare tubes of small diameter is used instead of conventional finned tubes [10]. The compact countercurrent cross-flow heat exchanger using small bare tubes of SUS304 was designed and constructed to prove its high ability. The outer and inner diameters of the bare tube were 10.5 and 8.5mm, respectively. The experimental study varying the steam concentration of

mixture gas, feed water temperature and flow rate was conducted.

## 2. EXPERIMENTAL APPARATUS AND METHOD

Shown in Fig.1 is a schematic of experimental apparatus. Steam and air were supplied from a boiler and a compressor, respectively, and well mixed before the test heat exchanger. The mixture gas was led to the upper plenum and flowed downward in the heat exchanger. The mixture gas was released to atmosphere from the outlet plenum. The supplied steam temperature was approximately 120°C and mixed with air of room temperature.

Shown in Fig.2 is the arrangement of heat transfer tubes. The heat exchanger consists of a staggered bank of 10(9) row tubes and 40 stages in total. The 10(9) tubes at each stage are connected with a header to maintain the same flow rate of feed water. The outer and inner diameters of the tube were 10.5 and 8.5mm, respectively. The feed water was supplied at the downstream of gas flow and flows counter-currently to the upstream. The temperature distributions of water and flue gas in the heat exchanger were measured with sheathed thermocouples. The thermocouple signals were transferred to a personal computer with a GPIB line and analyzed. The measurement error of the temperature in this study was within ±0.1 K. The pressure loss and the total amount of condensate generated in the heat exchanger were also measured.

The parametric study varying the flue gas flow rate, feed water temperature and flow rate was conducted. The major test conditions are shown in Table.1. The cooling water flow rate and temperature were maintained approximately at 600kg/h and 10°C, respectively. The steam mass flow rate was varied between 21 to 87 kg/h and the air mass flow rate was controlled to obtain a desired air mass concentration between 0 and 0.8. As the result of mixing of steam and air, the mixture gas temperature was between 80 and 113 °C.

## 3. CONSTITUTIVE EQUATIONS FOR PREDICTION

### 3.1 Heat resistance of condensate

Though a part of condensate falls down between the tubes and on the duct wall, it is assumed that all the condensate generated at the upper stage flows on the tubes as a laminar film. The momentum balance dominated by viscous and gravity force gives the velocity distribution at  $\theta^\circ$  from the tube top in Fig.3. :

$$u = \frac{(\rho_L - \rho_G)g \sin \theta}{\mu_L} \left( y\delta - \frac{y^2}{2} \right) \quad (3)$$

Integrating the above velocity profile and using the condensate mass flow rate per unit of tube length,  $m$ , yields

$$\delta = \left[ \frac{1.5\mu_L m}{\rho_L(\rho_L - \rho_G)g \sin \theta} \right]^{1/3} \quad (4)$$

The heat conductivity of film is

$$K = \frac{\lambda_L}{\delta} = \left[ \frac{\lambda_L^3 \rho_L (\rho_L - \rho_G) g \sin \theta}{1.5\mu_L m} \right]^{1/3} \quad (5)$$

Equation (5) gives the heat flux through the film when the

temperature difference between the film is multiplied. The average conductivity from  $\theta=0^\circ$  to  $\theta=\pi$  is

$$\bar{K} = \frac{1}{\pi} \int_0^\pi K d\theta = 0.72 \left[ \frac{\lambda_L^3 \rho_L (\rho_L - \rho_G) g}{\mu_L m} \right]^{1/3} \quad (6)$$

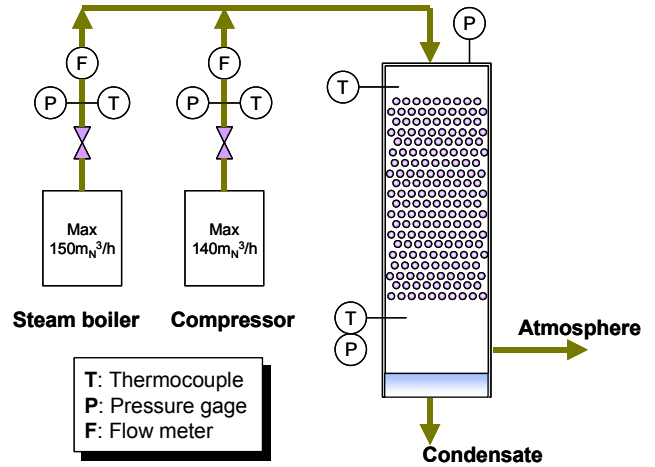


Fig. 1 Schematic of experimental apparatus

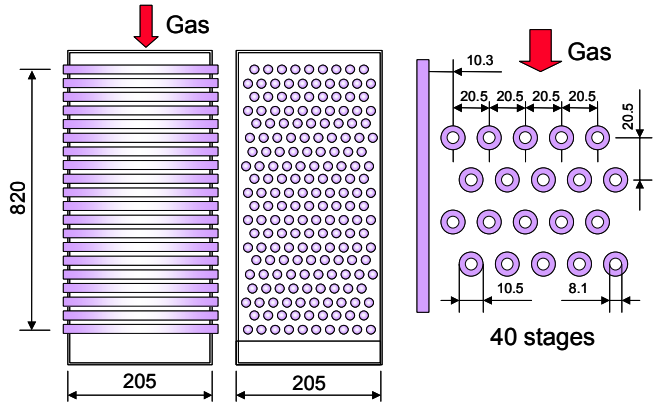


Fig. 2 Schematic of tube bank

Table1 Major test conditions

Steam mass flow rate kg/h	21.6 ~ 86.9
Air mass ratio 1 - $W_f$	0 ~ 0.8
Mixture gas temp. $T_f$ (°C)	80.6 ~ 113.2
Cooling water flow rate kg/h	592 ~ 614
Inlet temp. of cooling water (°C)	8.7 ~ 12.2

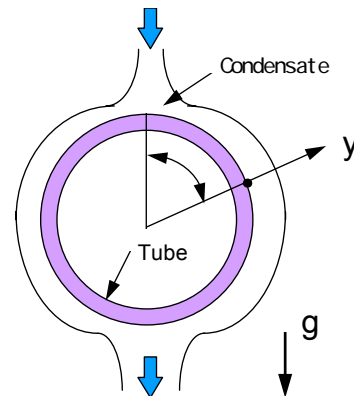


Fig. 3 Heat resistance of condensate film

The average heat resistance of film is defined as the inverse of the above average conductivity. The average film thickness is

$$\bar{\delta} = \frac{\lambda_f}{K} \quad (7)$$

In the calculation, the mass flow rate,  $m$ , at a certain stage includes the condensate generated at the stage for the conservative estimation.

### 3.2 Heat and mass transfer in gas side

The total heat flux  $q_w$  consists of the convection heat flux  $q_V$  and the condensation heat flux  $q_C$  as

$$q_w = q_V + q_C \quad (8)$$

The convection heat flux is expressed as

$$q_V = h(T_f - T_i) \quad (9)$$

The condensation heat flux  $q_C$  can be expressed as,

$$q_C = h_C L_W \rho_f (w_f - w_i) \quad (10)$$

where  $W_i$  is the mass concentration of saturated steam at the wall temperature  $T_i$ . Based on the previous studies[12], the Nusselt number  $Nu_f$  for the average convective heat transfer coefficient in the range of  $10^3 < Re_f < 2 \times 10^5$  is

$$Nu_f = c Re_f^a Pr_f^b (Pr_f / Pr_w)^{0.25} \quad (11)$$

Zukauskas[12] proposed  $a=0.6$ ,  $b=0.36$  and

$$\text{For } S_1/S_2 < 2 \quad c = 0.35(S_1 / S_2)^{0.2} \quad (12)$$

$$\text{For } S_1/S_2 \geq 2 \quad c = 0.40 \quad (13)$$

for a staggered bank. For the condensation of steam on heat transfer tubes, the modified analogy relation of Eqs.(1) and (2) gives

$$Sh_f = M_f c Re_f^a Sc_f^b (Sc_f / Sc_w)^{0.25} \quad (14)$$

where  $M_f = \frac{\text{Max}(1, 2 - 1.2\omega)}{1 - w_i} \left(\frac{1}{\omega}\right)^b$

The Sh number increases sharply at the steam mass concentration of 1 in Eq.(14). This indicates the mass transfer at the pure steam condition is enough high to neglect the interfacial resistance of mass transfer. In the calculation for pure steam without air, modification factor  $M_f$  of 100 was used to avoid the calculation error divided by zero.

Mixture gas was treated as a mixture of  $N_2$ ,  $O_2$  and  $H_2O$  and its property was estimated with special combinations of each gas property proposed by the previous studies. For example, the heat conductivity and the viscosity were estimated with the methods by Lindsay&Bromley [14] and Wilke[15], respectively. It is considered that a strong correlation exists between the thermal and mass diffusivities. As a first attempt, the mass diffusivity of steam in mixture gas was estimated with the well-known mass diffusivity of steam in air as

$$D = D_{air} \left( \frac{\kappa}{\kappa_{air}} \right) \quad (15)$$

where  $\kappa$  and  $\kappa_{air}$  are the thermal diffusivities of flue gas and dry air, respectively. The diffusivity of steam in air can be expressed as[16],

$$D_{air} = 7.65 \times 10^{-5} \frac{(T + 273.15)^{11/6}}{P} \quad (16)$$

The one-dimensional heat and mass balance calculation along the flow direction of flue gas was conducted. The steam mass concentration and the flue gas temperature at  $N+1$ th stage can be calculated from those at  $N$ th stage as shown in Fig.4.

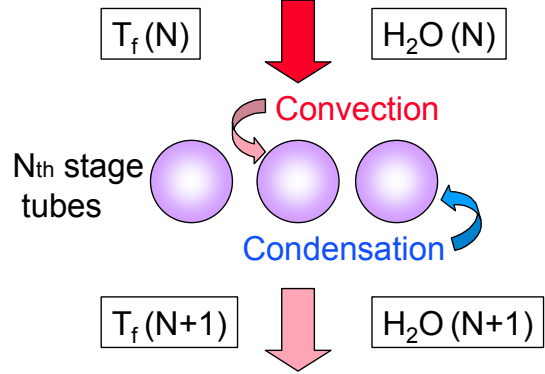


Fig. 4 One-dimensional calculation

The heat and mass balance equations are;

$$H_2O(N+1) = \frac{H_2O(N) \cdot V - \frac{q_C A_W}{L_W} \cdot \frac{22.4}{18}}{V - \frac{q_C A_W}{L_W} \cdot \frac{22.4}{18}} \quad (17)$$

$$T_f(N+1) = T_f(N) - \frac{q_V A_W}{C_{Pf} \rho_f (273.15 + T_f) / 273.15 \cdot V} \quad (18)$$

where  $A_w$  is the heat transfer area per a stage.

It is possible that the gas temperature merges with the dew point which is the saturation temperature corresponding to the partial pressure of steam in the flue gas. When the gas temperature decreases below the dew point, the condensation of steam in the flue gas takes place and the latent heat increases the gas temperature until the gas temperature coincides with the dew point. In this case, the energy balance gives the relation between the increase of the gas temperature,  $\Delta T_f$ , and the decrease of steam concentration,  $\Delta H_2O$ , as;

$$\Delta T_f = \frac{18}{22.4} \cdot \frac{L_W}{C_{Pf} \rho_f (273.15 + T_f) / 273.15} \cdot \Delta H_2O \quad (19)$$

### 3.3 Heat conduction in tube

The heat conductivity for the inconel or austenite stainless steel is given with the following approximate correlation [17].

$$\lambda_t = 13.2 + 0.013T_t \quad \text{W/(m K)} \quad (20)$$

where  $T_t$  is the average temperature of tube as,

$$T_t = \frac{T_w + T_{wi}}{2} \quad (21)$$

where  $T_w$  and  $T_{wi}$  are the outer and inner wall temperatures, respectively. The heat flux at the outer wall is,

$$q_w = \frac{2\lambda_t(T_w - T_{wi})}{d_o \ln(d_o/d_i)} \quad (22)$$

### 3.4 Heat transfer in water side

Heat transfer correlation by Dittus-Boelter taking account of the pipe inlet region is used. The coefficient by McAdams[18] was used for the modification.

$$Nu = 0.023 Re^{0.8} Pr^{0.4} \left(1 + \left(\frac{d_i}{L}\right)^{0.7}\right) \quad (23)$$

where L is the heating length of tube.

## 4. COMPARISON OF EXPERIMENTAL RESULT AND PREDICTION

### 4.1 Temperature distribution

Shown in Fig.5 is the comparison of the experimental result and the air mass concentration of 0.8. Feed water and steam mass flow rates were 600 and 22 kg/h, respectively. The key and are the measured temperatures of gas and water, respectively. The solid lines are the temperatures of gas and water in the tube bank. The a-dot-dashed line and the two-dots-dashed line are the interfacial temperature of condensate and the inner wall temperature of tubes, respectively. The dashed line which is the saturation temperature (dew point) corresponding to the partial pressure of steam in the flue gas agrees well with the gas temperature. As the outer wall temperature is smaller than the dew point, the condensation on the wall takes place throughout the heat exchanger. The dew point and gas temperature decrease with increasing stages as the steam concentration decreases. The prediction for the water temperature agrees well with the experimental result. The prediction for the gas temperature is slightly higher than the experimental result in the tube bank. In the present experiments, the entrained and dispersed condensate in the mixture gas tends to wet the thermocouples among the tube bank. The wet thermocouples indicate the lower value than the actual gas temperature.

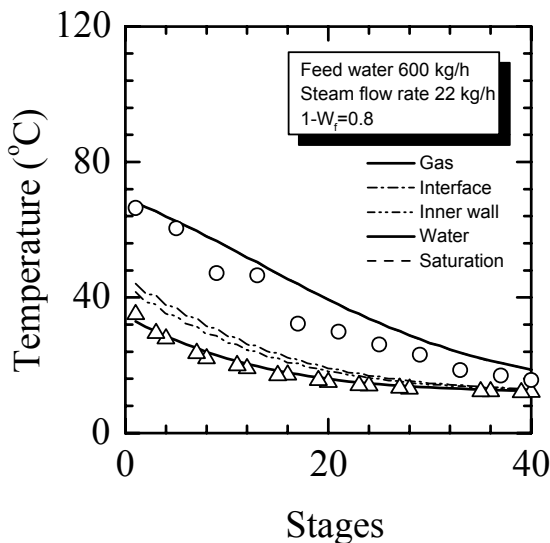


Fig. 5 Comparison of the experimental result and the prediction at air mass concentration of 0.8

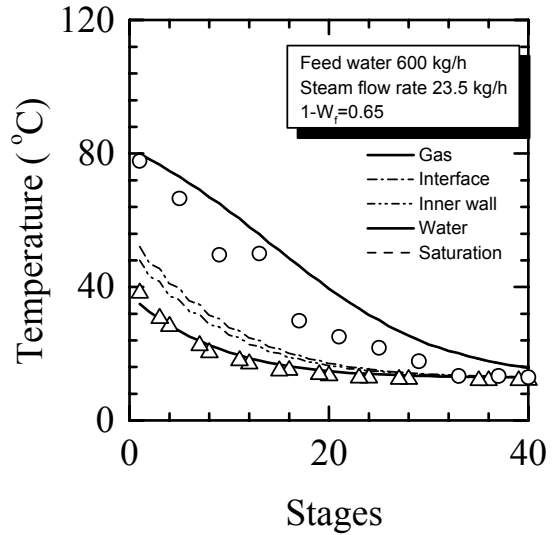


Fig. 6 Comparison of the experimental result and the prediction at air mass concentration of 0.65

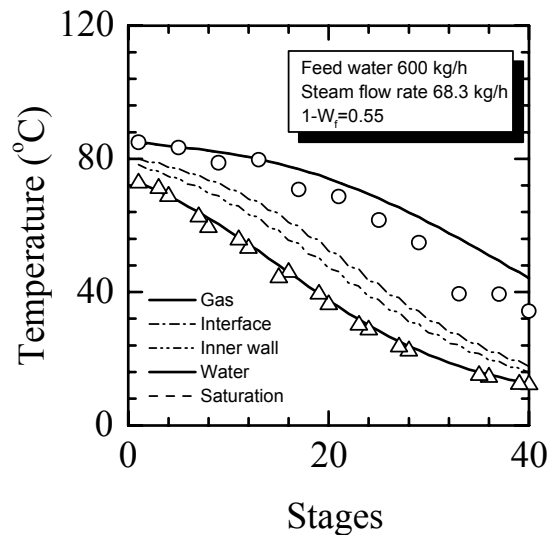


Fig. 7 Comparison of the experimental result and the prediction at air mass concentration of 0.55

The average thickness of condensate was calculated with the method mentioned above. It was assumed that all the generated condensate flows on the tubes in the calculation. The maximum thickness was approximately 0.1mm. The existence of the film did not affect the calculated temperature profiles in the bank. In the high air mass concentration, the effect of condensate film on the tubes was considered to be negligibly small for the heat and mass transfer calculation.

Shown in Figs.8 to 10 are comparisons of the experimental result and predictions when the air mass concentration was reduced. When the measurement locations of gas temperature were relatively high in the tube banks, the effect of the wet thermocouple is considered to be negligible. Generally the measured water temperature agrees well with the prediction.

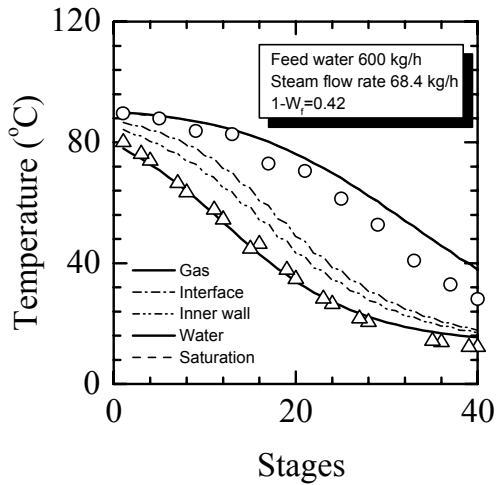


Fig. 8 Comparison of the experimental result and the prediction at air mass concentration of 0.42

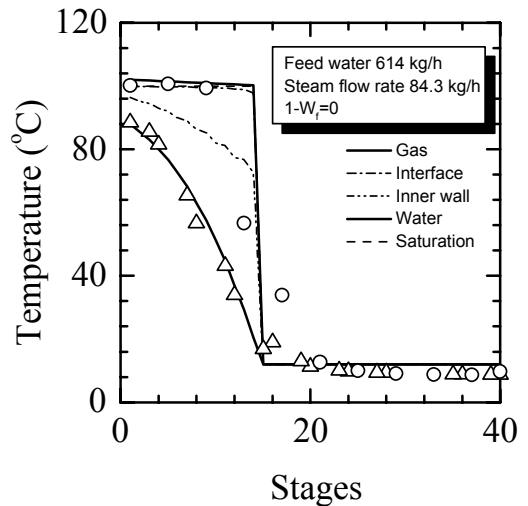


Fig. 11 Comparison of the experimental result and the prediction at pure steam

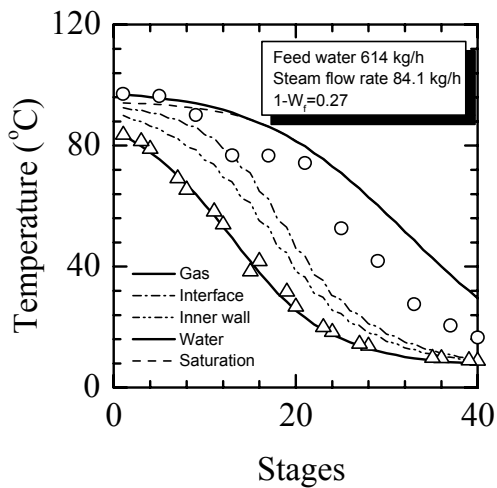


Fig. 9 Comparison of the experimental result and the prediction at air mass concentration of 0.27

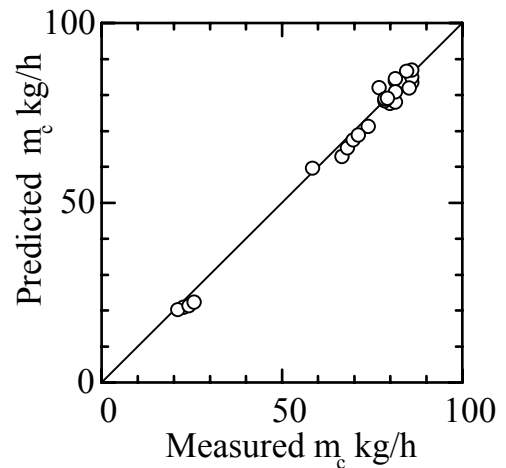


Fig. 12 Predicted and measured total amount of condensate

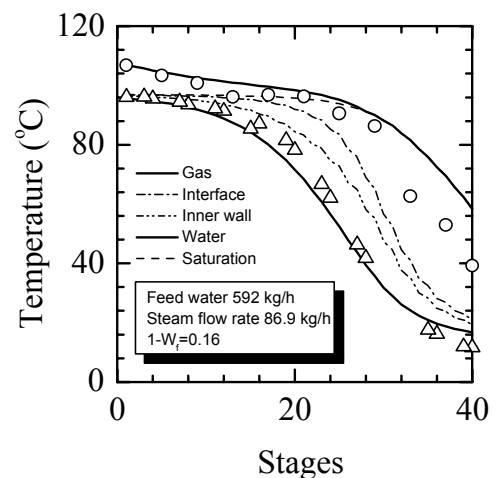


Fig. 10 Comparison of the experimental result and the prediction at air mass concentration of 0.16

When the air mass concentration was 0.16 in Fig.10, the heat transfer at the tubes near the inlet of mixture gas was strongly depressed as indicated with the graduate decrease of water temperature. The saturation temperature limited the interfacial temperature of condensate film and the heat transfer was depressed due to the small temperature difference between water and interface.

In the case of pure steam as shown in Fig.11, the interfacial temperature was equal to the saturation temperature. Heat resistance of condensate film governed heat transfer. When the gas temperature sharply dropped, all the steam had condensed above this height. Below the height, air could invade from the outlet of heat exchanger and the heat transfer was strongly depressed. Even in this case, prediction agrees well with the experiment.

#### 4.2 Amount of condensate

Shown in Fig.12 is the comparison of experimental result and prediction for the amount of condensate throughout the heat exchanger. The condensate was collected

at the bottom of heat exchanger and the amount was measured. The total amount of condensate generally agrees well with the present prediction.

## 5. CONCLUSION

The modified analogy relation considering the mass absorption effect on the condensing interface was used in the present prediction method for the condensing heat exchanger for exhaust gas from fuel cell. The experimental results for the temperature distributions of water and mixture gas in the compact heat exchanger with bare tubes of small diameter agreed well with the prediction. The measured total amount of condensate also agreed well with the present prediction. The prediction method was useful for the design of the heat exchanger in the wide range of steam concentration.

## NOMENCLATURE

$C_p$ : specific heat [J/kg]  
 $d$ : outer diameter of tube [m]  
 $d_i$ : inner diameter of tube [m]  
 $D$ : mass diffusivity [ $m^2/s$ ]  
 $h_v$ : heat transfer coefficient [ $W/(m^2K)$ ]  
 $h_c$ : mass transfer coefficient [m/s]  
 $L_w$ : latent heat [J/kg]  
 $Nu$ : Nusselt number [ $= h_v d / \lambda$ ]  
 $P$ : pressure [Pa]  
 $q$ : heat flux [ $kW/m^2$ ]  
 $Pr$ : Prandtl number [ $= \nu / \kappa$ ]  
 $Re$ : Reynolds number [ $= ud / \nu$ ]  
 $S_1$ : spanwise pitch [m]  
 $S_2$ : flow-directional pitch [m]  
 $Sh$ : Sherwood number [ $= h_c d / D$ ]  
 $Sc$ : Schmidt number [ $= \nu / D$ ]  
 $T$ : temperature [ $^{\circ}C$ ]  
 $u$ : velocity at minimum flow area [m/s]  
 $V$ : volumetric flow rate [ $m_N^3/s$ ]  
 $w$ : mass concentration per fluid of an unit mass [kg/kg]  
 $\kappa$ : thermal diffusivity [ $= \lambda / (\rho C_p)$ ]  
 $\lambda$ : heat conductivity [ $W/(mK)$ ]  
 $\nu$ : kinematic viscosity [ $m^2/s$ ]  
 $\rho$ : density [ $kg/m^3$ ]

## subscript

C: condensation  
 f: mixture gas  
 i: interface(condensation surface)  
 V: convection  
 W: total or wall of tube  
 N: standard condition at  $0^{\circ}C$  and atmospheric pressure  
 sat: saturated condition of steam

## REFERENCES

- Osakabe, M., Ishida, K., Yagi, K., Itoh, T. and Ohmasa, M., "Condensation heat transfer on tubes in actual flue gas (Experiment using flue gas at different air ratios)", (in Japanese), Trans. of JSME , 64-626, B, (1998), 3378-3383.
- Osakabe, M., Yagi, K., Itoh, T. and Ohmasa, M., "Condensation heat transfer on tubes in actual flue gas (Parametric study for condensation behavior)", (in Japanese), Trans. of JSME , 65-632, B, (1999), 1409-1416.
- Osakabe, M., Itoh, T. and Ohmasa, M., "Condensation heat transfer on spirally finned tubes in actual flue gas", (in Japanese), J. of MESJ , 35-4, (2000), 260-267.
- Osakabe, M., Itoh, T. and Yagi, K., "Condensation heat transfer of actual flue gas on horizontal tubes", Proc. of 5th ASME/JSME Joint Thermal Eng. Conf., AJTE99-6397, (1999).
- Osakabe, M., "Thermal-hydraulic behavior and prediction of heat exchanger for latent heat recovery of exhaust flue gas", Proc. of ASME, HTD-Vol.364-2, (1999), 43-50.
- Osakabe, M., Tanaka, O. and Kawakami, A., "Prediction and behavior of heat exchanger for latent heat recovery of exhaust flue gas", (in Japanese), Trans. of JSME, 66-649, B, (2000), 2471-2477.
- Osakabe, M., "Thermal-hydraulic behavior and prediction of heat exchanger for latent heat recovery of exhaust flue gas", Proc. of ASME, HTD-Vol.364-2, (1999), 43-50.
- Osakabe, M., "Latent heat recovery from oxygen-combustion flue gas", Proc. of 35th Intersociety Energy Conversion Conference, Vol.2, (2000), 804-812.
- Osakabe, M., Horiki, S., Itoh, T. and Mouri, K., "Latent Heat Recovery from Oxygen-Combustion Boiler", Proc. of RAN2001 (Nagoya), (2001).
- Osakabe, M., Horiki, S., Itoh, T. and Haze, I., "Latent Heat Recovery from Actual Flue Gas", Proc. of IHTC 12 (Grenoble), (2002).
- Osakabe, M. and Ikeda, N., to be published in Trans. of JSME.
- Zukauskas, A., Advances in Heat Transfer, 8, Academic press, New York, (1972), 93-160
- JSME, Data Book: Heat Transfer 3rd Edition, (in Japanese), 1983.
- Lindsay, A.L. and Bromley L.A., "Thermal conductivity of gas mixtures", Indust. Engng. Chem., 42, (1950), 1508-1510.
- Wilke, C.R., "A viscosity equation for gas mixture", J. Chem. Phys., 18, (1950), 517-519.
- Fujii, T., Kato, Y. and Mihara, K., "Expressions of transport and thermodynamic properties of air, steam and water", Univ. Kyushu Research Institute of Industrial Science Rep.66, (1977), 81-95.
- Osakabe, M., "Thermal-hydraulic study of integrated steam generator in PWR", J. Nucl. Sci. & Technol., 26(2), (1989), 86-294.
- McAdams, W.H., Heat transmission, McGRAW-HILL, (1954).